Opto-Electronic Advances

CN 51–1781/TN ISSN 2096–4579 (Print) ISSN 2097–3993 (Online)

Adaptive decentralized AI scheme for signal recognition of distributed sensor systems

Shixiong Zhang, Hao Li, Cunzheng Fan, Zhichao Zeng, Chao Xiong, Jie Wu, Zhijun Yan, Deming Liu and Qizhen Sun

Citation: Zhang SX, Li H, Fan CZ, et al. Adaptive decentralized AI scheme for signal recognition of distributed sensor systems. *Opto-Electron Adv* **7**, 240119(2024).

https://doi.org/10.29026/oea.2024.240119

Received: 20 May 2024; Accepted: 6 August 2024; Published online: 29 September 2024

Related articles

Opto-Electronic Advances

Article

December 2024, Vol. 7, No. 12

DOI: 10.29026/oea.2024.240119 CSTR: 32247.14.oea.2024.240119

Adaptive decentralized AI scheme for signal recognition of distributed sensor systems

Shixiong Zhang[1], Hao Li[1], Cunzheng Fan[1], Zhichao Zeng[1], Chao Xiong[5], Jie Wu[6], Zhijun Yan[1,3,4], Deming Liu[1] and Qizhen Sun[1,2,3,4]*

Artificial intelligence (AI) plays a critical role in signal recognition of distributed sensor systems (DSS), boosting its applications in multiple monitoring fields. Due to the domain differences between massive sensors in signal acquisition conditions, such as manufacturing process, deployment, and environments, current AI schemes for signal recognition of DSS frequently encounter poor generalization performance. In this paper, an adaptive decentralized artificial intelligence (ADAI) method for signal recognition of DSS is proposed, to improve the entire generalization performance. By fine-tuning pre-trained model with the unlabeled data in each domain, the ADAI scheme can train a series of adaptive AI models for all target domains, significantly reducing the false alarm rate (FAR) and missing alarm rate (MAR) induced by domain differences. The field tests about intrusion signal recognition with distributed optical fiber sensors system demonstrate the efficacy of the ADAI scheme, showcasing a FAR of merely 4.3% and 0%, along with a MAR of only 1.4% and 2.7% within two specific target domains. The ADAI scheme is expected to offer a practical paradigm for signal recognition of DSS in multiple application fields.

Keywords: artificial intelligence (AI); signal recognition; distributed sensor systems (DSS); distributed optical fiber sensors (DOFS)

Zhang SX, Li H, Fan CZ et al. Adaptive decentralized AI scheme for signal recognition of distributed sensor systems. *Opto-Electron Adv* **7**, 240119 (2024).

Introduction

Distributed sensor systems (DSS) consist of multiple sensors that can monitor various parameters such as acoustic wave, temperature, and strain, whose implementation forms include sensor network[1], and sensor array[2–4], etc. The signal recognition of DSS necessitates the processing of massive and complex data[5,6]. By learning patterns from massive existing data without explicit modeling, AI can enable real-time processing and robust recognition in various fields of DSS[7,8], such as realizing movement recognition and vital signs monitoring in wearable applications[9], improving diagnostic result quality in industrial fault detection[10], detecting raw water quality in environmental monitoring[11], and classifying the healing versus nonhealing status of wound in medical applications[12].

An important factor that limits the application of DSS is the poor generalization of AI models on massive

[1]School of Optical and Electronic Information, National Engineering Research Center of Next Generation Internet Access-system, Huazhong University of Science and Technology, Wuhan 430074, China; [2]PGMF and School of Physics, Huazhong University of Science and Technology, Wuhan 430074, China; [3]Jinyinhu Laboratory, Wuhan 430048, China; [4]Optics Valley Laboratory, Wuhan 430074, China; [5]Nanjing Research Institute of Electronic Equipment, Nanjing 210007, China; [6]Wenzhou Quality and Technology Testing Research Institute, Wenzhou 325000, China.

*Correspondence: Q Z Sun, E-mail: qzsun@mail.hust.edu.cn

Received: 20 May 2024; Accepted: 6 August 2024; Published online: 29 September 2024

sensors, which is caused by the data distribution differences between different sensors and insufficient training data[13]. Specifically, massive sensors are inevitably distributed in multiple domains where signal acquisition conditions are diverse, such as manufacturing process, deployment, and environments, etc. The corresponding sensing signals will exhibit differences in data distribution, further leading to poor generalization performance when using the same AI model for all domains[14]. To tackle this problem, massive labeled data from each domain is needed to train the corresponding model, but it is not cost-effective when there are many domains. Thus, how to fully utilize the existing data for model training to improve generalization performance in each domain, has become a common goal[15]. The existing data mainly comes from source domain and each target domain[16]. The target domain refers to the domain where recognition task will be carried out, in which labeled data is available and unlabeled data can be acquired automatically. While, the source domain can provide additional labeled data and pre-trained model. Due to the differences in types of existing data in various fields of DSS, corresponding researchers have different data utilization methods. To improve efficacy of crack identification, the synthetic data generated by a finite element model in target domain is used to train recognition model by supervised learning (SL) method[17]. Then, the data of hand movement sampled by nanomesh sensors in target domain is used by unsupervised learning (UL) method, to realize data-efficient of gesture recognition[18]. Additionally, to improve earthquake detection performance, the conventional seismic data recorded by seismic networks in source domain and the acoustic data acquired by distributed acoustic sensors in target domain are utilized by semi-supervised learning (SSL) method[7]. Due to the underutilization of the potential properties and available information of unlabeled data from all domains, these studies encounter difficulties in specifying adaptive recognition schemes for each domain, which needs to optimize data utilization method for the improvement of model generalization performances.

Distributed optical fiber sensor (DOFS), as a typical type of DSS, performs sensing by demodulating the changes in optical signals[19]. Assisted with AI technology, DOFS has performed various tasks about signal recognition, such as recognizing signals of ships and marine organisms with CNN in ocean monitoring[20], pre-warning the intrusion signals with support vector machine in structure health monitoring[21], and detecting integrity threats with Hidden Markov Models in pipelines monitoring[22,23]. Due to the domain differences in signal acquisition conditions, such as geographic conditions, fiber coupling status, and noise in environment and system, the intrusion signal recognition of DOFS faces the problem of high false alarm rate (FAR) and missing alarm rate (MAR). To solve this problem, existing researches pursue better data utilization methods, which can be divided into three categories: information extraction of labeled data from target domain, information mining of unlabeled data from target domain, and knowledge exploitation of pre-trained model from source domain. The labeled data in target domain contains the abundant information, and many researchers focus on the SL methods[24]. These studies pursue effective features and strong classifiers, and utilize data augmentation methods to expand dataset, such as Conditional GAN and Cycle-GAN[25–27]. These methods extracted valuable information from acquired labeled data, while they still need adequate labeled data in each target domain. Once DOFS system has been installed in practical applications, massive unlabeled data will be continuously generated in each target domain. Traditional SL methods are unable to utilize the unlabeled data. Thus, researchers shifted their focus towards the UL and SSL methods[28–30]. Among them, unsupervised spiking neuron network is used to extract information of unlabeled data[31], Fixmatch method is employed to train model with pseudo-labeled data[32], and the auto-encoder (AE) model is pretrained with unlabeled data[33]. The above methods only mine data information from target domain, which can be improved by exploring knowledge from source domain. Some researchers pre-trained the model on existing dataset from source domain and then fine-tuned it with labeled data from target domain[34,35], while they still lack utilization of the unlabeled data from each target domain. Thus, a gap in existing research is to establish a model transferring scheme that can utilize data from all domains, reducing overall FAR and MAR by adapting each transferred model to corresponding domain.

In this paper, an adaptive decentralized AI (ADAI) scheme for signal recognition of DSS is proposed. By utilizing the existing data from all domains, ADAI scheme trains a series of adaptive AI models for all target domains, which can improve generalization performance of the entire DSS. For the model training in a specific target domain, ADAI scheme employs domain adaptation

(DA) to bridge the labeled data from source domain and unlabeled data from this target domain, achieving the historical models at different training epochs. Then, the ensemble pseudo labeling (EPL) method is proposed to label the unlabeled data, selecting the most adaptive model from historical models. Notably, ADAI scheme performs significantly in reducing the FAR and MAR, even when the available unlabeled dataset contains only negative samples. To verify the effectiveness of the ADAI scheme, this paper takes the DOFS system for intrusion signal recognition as an example. Since ADAI scheme targets the common issues of utilizing unlabeled data to reduce data distribution differences between multiple sensors, this work is also applicable to other fields of DSS.

Method

Adaptive decentralized artificial intelligence method

Since unlabeled data is sampled on the distribution of test data, it contains the intrinsic information about the corresponding domain, which can be reflected in the data distribution coverage. As shown in Fig. 1(a), although there is a certain gap between the distribution coverage of unlabeled data and test data in each domain, this gap will be narrowed as unlabeled data accumulates. This accumulation process is automatic when the DSS have been installed. As depicted in Fig. 1(b), the data distribution between different domains varies with the domain differences. The recognition ability of pre-trained model is limited to the data distribution in source domain (Domain-S), making it hard to cover the data distribution in target domains. Fortunately, the distribution of accumulated unlabeled data covers a portion of the distribution of test data, which can provide additional information. Thus, the ADAI scheme is proposed to fine-tune the pre-trained model with unlabeled data from each target domain, achieving the adaptive decentralized models that can cover the corresponding data distributions. ADAI scheme decomposes the decentralized model training task into a series of model transferring tasks from source domain to all target domains. Figure 1(c) illustrates the process of ADAI scheme on a model transferring task. ADAI scheme first fine-tunes the pre-trained model by DA method, achieving historical models at different training epochs. However, these historical models have diverse recognition coverages for the data distribution of a specific domain (Domain-T). Thus, ADAI scheme further employs the EPL method to select the most adaptive model from historical models for Domain-T.

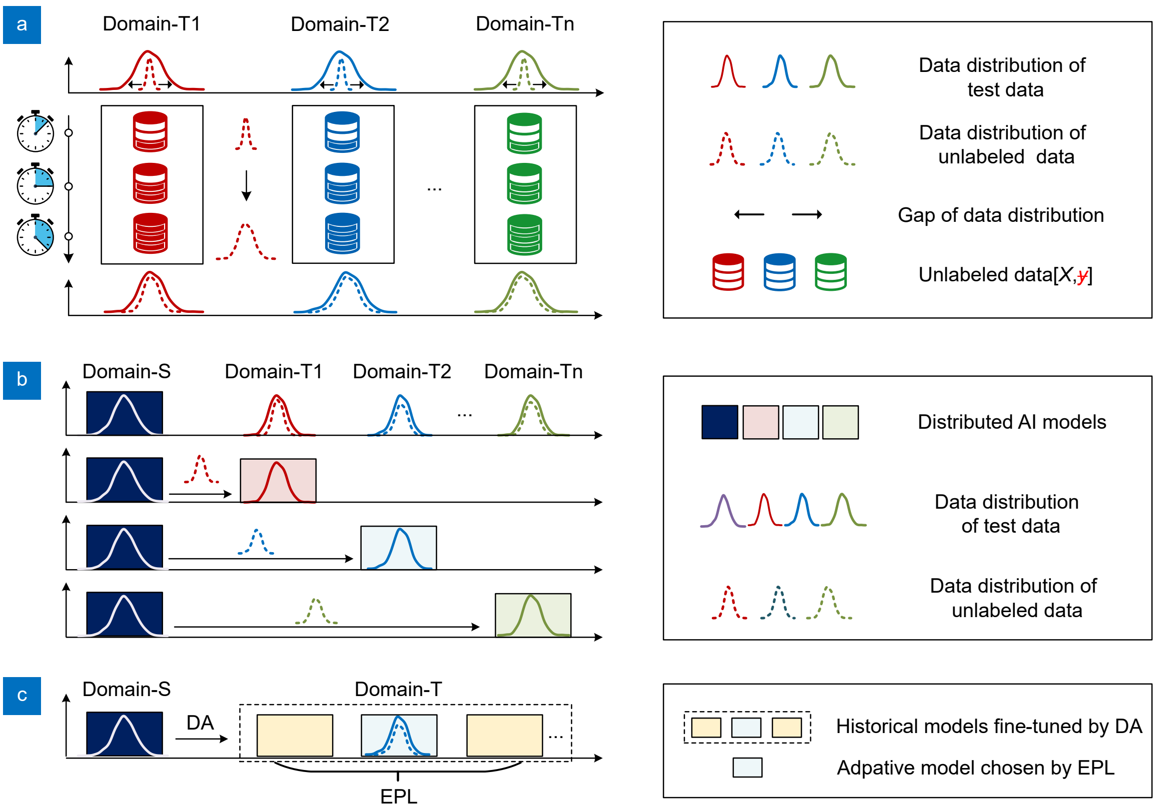

Fig. 1 | (**a**) The characteristics of unlabeled data. (**b**) The model transferring tasks by ADAI scheme. (**c**) The process of ADAI scheme.

Domain adaptation for model training

For the model transferring from Domain-S to Domain-T, test data from two domains are transformed through the feature extractor of pre-trained model, yielding feature distributions D_S and D_T. The data distribution difference caused by domain differences will map as the offset between D_S and D_T. It further leads to the poor performance with the classifier of pre-trained model in Domain-T. Specifically, the formula for error limit is utilized to explain this domain mismatch[36], which can be represented by:

$$\varepsilon_T(h) \leqslant \varepsilon_S(h) + \frac{1}{2} d_{H\Delta H}(D_S, D_T) + \lambda \ , \quad (1)$$

where $\varepsilon_T(h)$ represents the expected error of test data from Domain-T, which is limited by three terms on the right side of the inequality. The λ is a small constant, which is expected to be negligible. The $\varepsilon_S(h)$ represents the expected error of test data from Domain-S, and the $d_{H\Delta H}(D_S, D_T)$ denotes the offset between D_S and D_T. To reduce the upper limit of error $\varepsilon_T(h)$, DA method designs two loss functions of l_S and l_{S-T} to reduce $\varepsilon_S(h)$ and $d_{H\Delta H}(D_S, D_T)$, respectively. As shown in Fig. 2(a), l_S is the cross-entropy loss function that calculates the recognition error of model on labeled dataset from source domain (Dataset-S), and l_{S-T} is measured by the distance metric function of Local Maximum Mean Discrepancy (LMMD), which computes the weighted sum of distances for each class between Dataset-S and unlabeled dataset from target domain (Unlabeled dataset-T'). Compared with the Maximum Mean Discrepancy (MMD), LMMD mitigates the interference caused by data distribution differences between signals of different classes, making it a more precise method to measure the feature distribution offset[37,38]. The target loss function can be reformed by:

$$l = r_{S-T} \cdot l_{S-T}(D_S, D_T) + r_S \cdot l_S(y_S, \widehat{y_S}) \ , \quad (2)$$

where r_{S-T} and r_S are the ratios of $l_{S-T}(D_S, D_T)$ and $l_S(y_S, \widehat{y_S})$, respectively. The $\widehat{y_S}$ is the model output for sample in Dataset-S and y_S is the corresponding label vector. Through the optimization process with the target loss function l, models at different training epochs are achieved during model transferring from Domain-S to Domain-T.

Ensemble pseudo labeling method for model selecting

Historical models at different training epochs have different recognition performances on Domain-T. Thus, it generally needs a labeled dataset to evaluate model performance on loss or accuracy, selecting the most adaptive model. However, labeled data may be unavailable in target domains for signal recognition tasks that require cost control. Thus, it is necessary to establish a validation set by utilizing the existing unlabeled data and historical models. Pseudo labeling (PL) technology believes that the predicted labels of effective unlabeled samples can be used for model training, and it will be increasingly accurate as model iteratively optimizes[39,40]. Intuitively, the ensemble-based method can vote for a statistical optimal prediction based on historical models, and this prediction may be used for PL technology[41]. As shown in Fig. 2(b), the EPL method builds an ensemble model by combining historical models, and then uses its output to assign the original pseudo label y_T for unlabeled sample X_T. Subsequently, data cleaning is used to get pure pseudo labels $\bar{y}_T$. Finally, the $\bar{y}_T$ and X_T are combined as the effective sample $[X_T, \bar{y}_T]$ for validation set. The adaptive model with the highest accuracy on this validation set is selected from historical models.

A typical application of ADAI scheme: intrusion signal recognition with DOFS system

As a typical type of DSS, DOFS system can acquire spatio-temporal acoustic signals over hundreds of kilometers using a single fiber. As shown in Fig. 3, the intrusion signal recognition of DOFS system is applied in scenes of

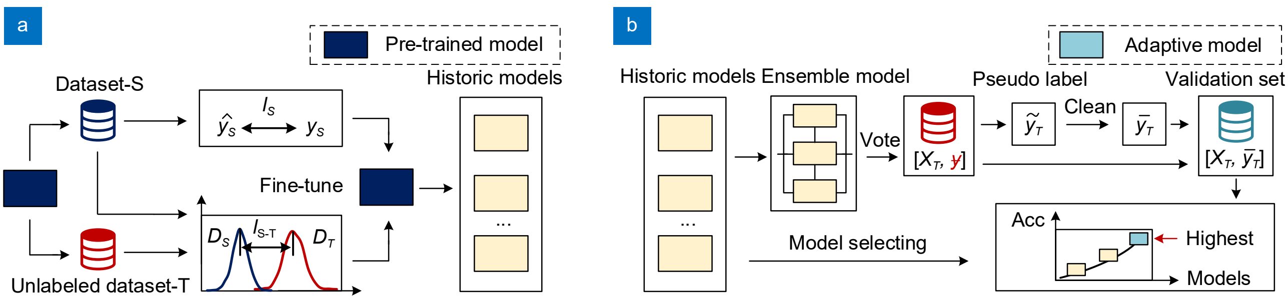

Fig. 2 | The detailed process of ADAI scheme. (**a**) The model training by DA method. (**b**) The model selecting by EPL method.

underground structure monitoring (Domain-T2), pipe monitoring (Domain-T1), and perimeter security (Domain-S). Optical fiber is attached near the monitoring structure, to acquire surrounding acoustic signals. The acoustic signals in different scenes are recognized by AI algorithm, detecting the potential intrusion events. However, sensing fiber will pass through various domains within evolving and complicated signal acquisition conditions, such as geographic environments, fiber coupling states, background noises, event action modes, etc. Additionally, the optical devices in sensing system have time-varying noise, and the different parts of fiber have diverse backscattering effects due to the differences in manufacturing processes. These differences will cause data distribution differences across each domain, and further lead to the high FAR and MAR when using the same model for all domains. Thus, the intrusion signal recognition of DOFS system is a typical application of DSS, which is suitable for verifying the effectiveness of ADAI scheme. Intuitively, the unlabeled dataset in each domain contains intrinsic information about the corresponding domain, such as static acquisition information and dynamic response information of intrusion signals. Based on these intrinsic information, ADAI scheme fine-tunes pre-trained model AI-S with the unlabeled dataset from each target domain and existing labeled data, achieving the adaptive decentralized AI models (AI-T1 and AI-T2) for all target domains. Compared with AI-S, AI-T1 and AI-T2 are more suitable for intrusion recognition in Domain-T1 and Domain-T2.

Experimental settings

Experimental scenes

To validate the robustness of ADAI scheme for intrusion signal recognition task in three domains, the intrusion signals monitoring system assisted with distributed acoustic sensing (DAS) technology is utilized for field tests. As a type of DOFS technology, DAS technology has the advantages of high signal fidelity and accurate positioning, making it suitable for intrusion signal recognition task[42]. As shown in Fig. 4(a), four typical events including background noise, vehicle driving, manual knocking, and excavator are monitored in three domains, labeled as 0, 1, 2, and 3, respectively. The scenes of Domain-S, Domain-T1, and Domain-T2 are perimeter, factory pipelines, and underground tunnel, respectively. The fiber in Domain-S is buried in clay and the event model is relatively single. To ensure the diversity in geographical environment and fiber coupling state, the fiber in Domain-T1 passes through sand, clay, and drain. Furthermore, the events in Domain-T2 have different event action modes: vehicle driving (car and truck), manual knocking (digging and jumping on the ground), and excavator (scrapping and hitting). The demodulated waveforms of four events in three domains are shown in Fig. 4(b). For all waveforms, the horizontal and vertical

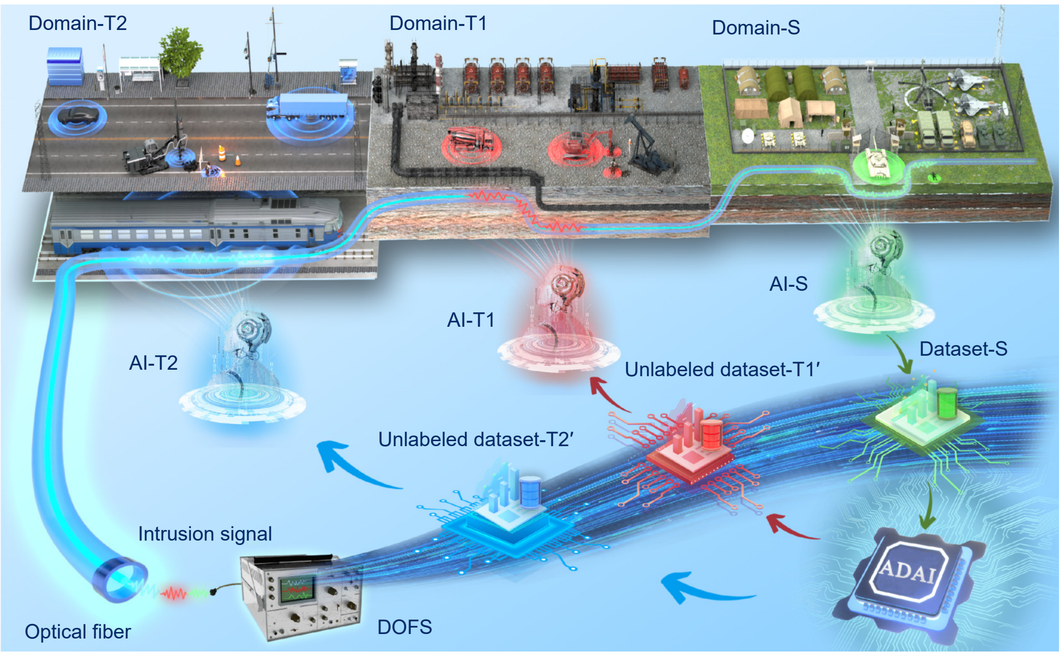

Fig. 3 | A typical application of ADAI scheme about intrusion signal recognition with DOFS system.

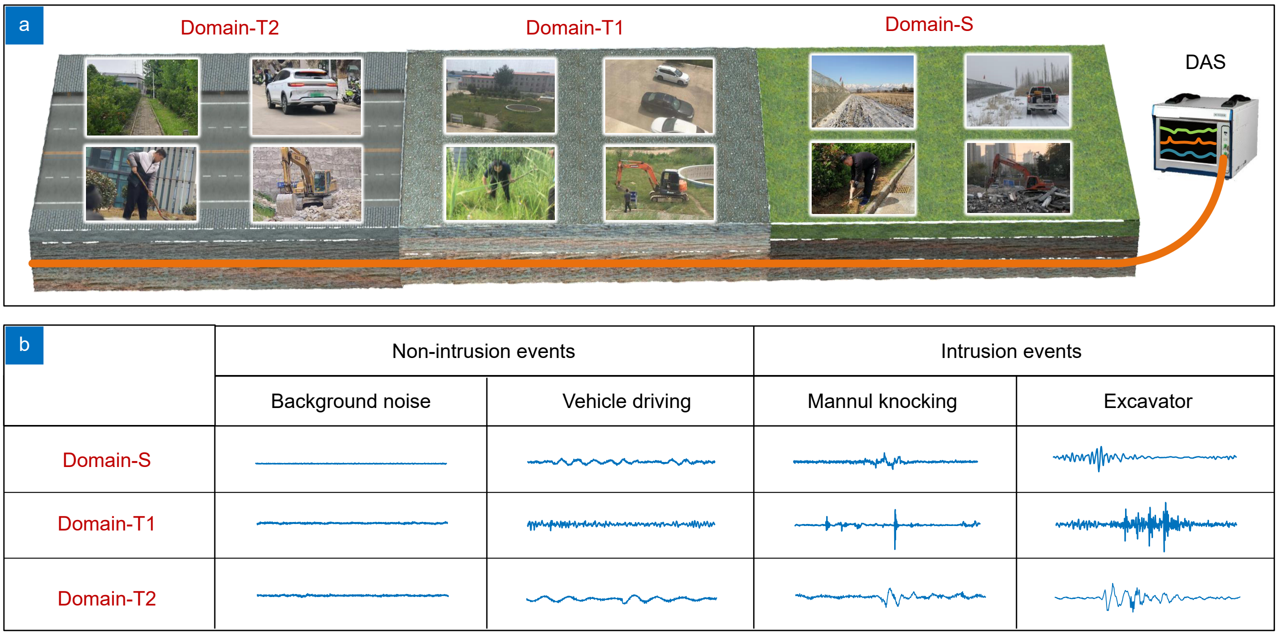

Fig. 4 | (**a**) The experimental scenes of three domains. (**b**) The demodulated waveforms of four typical events in three domains.

axes represent time and amplitude, which are both scaled within the same interval. Due to differences in signal acquisition conditions, the same type of signals may present different waveforms, which may be confused with other types of signals.

Dataset information

Table 1 illustrates the details of dataset information in three domains. Dataset-S, Dataset-T1, and Dataset-T2 are all labeled datasets from Domain-S, Domain-T1, and Domain-T2. The Unlabeled dataset-T1' and Unlabeled dataset-T2' are datasets whose labels are removed during the model training. Although the event types of two unlabeled datasets are limited to 0 and 1 in this work, their waveforms still contain the intrinsic information about corresponding domain. The data of background noise contains static acquisition information, such as the noise distributions in DAS system and external environment. Additionally, the data of vehicle driving can provide dynamic response information, such as geographical conditions and fiber coupling status. Thus, the unlabeled dataset can provide additional information for model transferring.

Settings of model training

The architecture of AI model is shown in Fig. 5. The input and output are one-dimensional sample and event type, whose shape are 1×1000 and 4, respectively. Transition block includes layers of batch normalization (BN), ReLU, convolution (Conv), and average pooling (Avg Pool). Dense block is composed of layers of BN, ReLU, and Conv. Bottleneck layer is achieved with 1×1 Conv. Noted that the layers from Conv+Pool to bottleneck layer are combined as the feature extractor, where the feature distribution is achieved.

Methods comparison

Baseline is the method without any operation on the pre-trained model. The Fixmatch and AE are two typical semi-supervised methods[43,44]. They perform well in the applications of DOFS, which are replicated for comparison

Table 1 | Details of dataset information.

	Non-intrusive events		Intrusion events	
	Background noise (0)	Vehicle driving (1)	Manual knocking (2)	Excavator (3)
Dataset-S	2054	2248	462	2121
Dataset-T1	900	378	857	329
Dataset-T2	983	463	117	1604
Unlabeled dataset-T1'	1224 = 1000 (0) + 224 (1)		-	-
Unlabeled dataset-T2'	1465 = 1000 (0) + 465 (1)		-	-

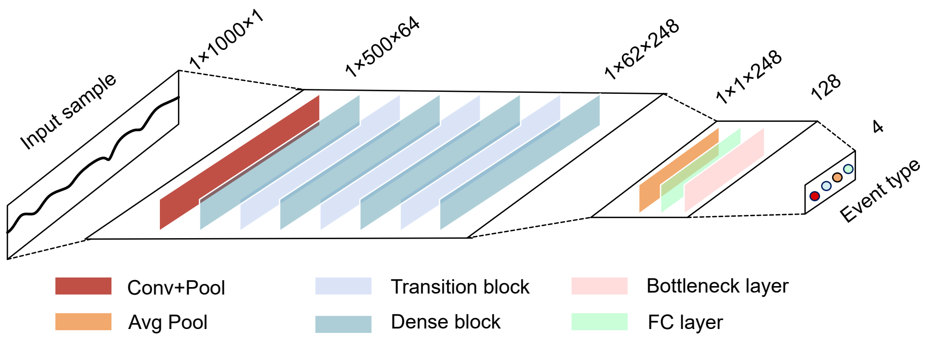

Fig. 5 | The architecture of AI model.

in this paper[32,33]. Compared with the methods of AE and Fixmatch, ADAI has the improvements of better loss function, EPL module for model selecting and decentralized AI training. The loss functions of AE and Fixmatch only calculate mapping loss and pseudo-labeled loss on unlabeled data in target domain, while the ADAI calculates the loss of labeled data in source domain and the offset loss between labeled data in source domain and unlabeled data in target domain, which can effectively learn all the existing information. The EPL module in ADAI can establish a pseudo-labeled validation set to select the adaptive model by PL technology and ensemble-based method, which is not available in AE and Fixmatch. The existing researches only discuss about semi-supervised learning in a specific domain. However, the decentralized AI training can achieve adaptive models for each domain, which will improve the recognition accuracy of the entire system.

Model naming

Different datasets and methods will achieve different recognition models. Thus, the naming rule for models is established as follows: Model - (method) – (dataset-1) – (dataset-2). When using DA method to fine-tune the pre-trained model with Dataset-T1', the Model-(DA)-T1' at different training epochs will be achieved. Among them, the best model selected by EPL method is named as the Model-(ADAI)-T1'. Besides, the Model-(ADAI)-T1' trained with Dataset-T1 will be named as the Model-(ADAI)-T1'-T1.

Results and discussion

Model transferring process of ADAI scheme

Model training by DA method

Without labeled data from Domain-T1, the Unlabeled dataset-T1' is employed to fine-tune the Model-(Baseline), achieving the Model-(DA)-T1' and Model-(Fixmatch)-T1'. Since there is no labeled dataset available for model validation, Unlabeled dataset-T1' is labeled here. As shown in Fig. 6(a), the recognition accuracies of Model-(Fixmatch)-T1' are unstable both on Dataset-S and Unlabeled dataset-T1', and they drop shapely at the end of training epochs, which is attributed to the instability of model classification ability. By contrast, as the training progresses, the recognition accuracies of Model-(DA)-T1' on two datasets tend to be stabilized. It indicates that DA method not only adapts the model to target domain, but also maintains the model classification ability. Then, the accuracies of Model-(DA)-T1' on two datasets at the 1~10 training epochs are visualized in Fig. 6(b). During the first four training epochs, the accuracy changes of two curves exhibit an opposing trend. This discrepancy occurs because the DA method is narrowing the feature distribution offset between two domains at the early stages of training. In the following training epochs, two curves represent the same changing trend. This convergence proves that the Model-(DA)-T1' can filter out the interference of feature distribution offset and improve its recognition accuracies in both domains. However, this model adaptation process is invisible in the model training by Fixmatch method. As shown in Fig. 6(c), two curves have the similar changing trend and they both drop shapely at some epochs, which indicates that its model training process is in a chaotic situation. Overall, DA method is more stable than Fixmatch method when fed with Unlabeled dataset-T1'.

Model selecting by EPL method

Although the DA method improves the recognition ability of AI models in Domain-T1, it is unable to select the most adaptive model without labeled dataset. Once the accuracy curve fluctuates greatly along the epoch axis, the model selecting will be difficult. To address this limitation, the EPL method is employed to create a pseudo-label

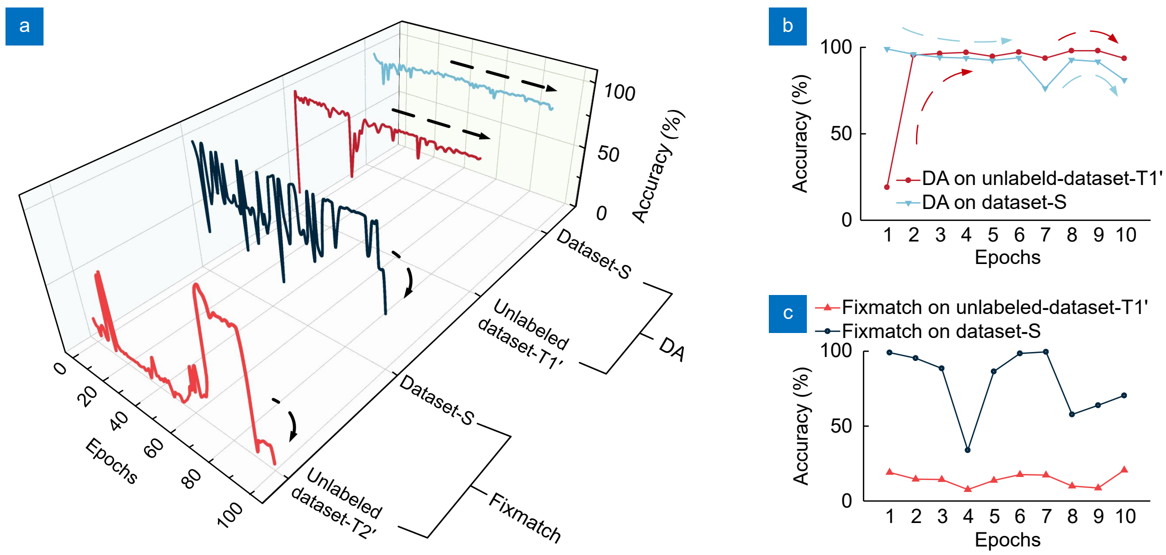

Fig. 6 | (a) The recognition accuracies of Model-(DA)-T1' and Model-(Fixmatch)-T1' on Dataset-S and Unlabeled dataset-T1' at different training epochs. The recognition accuracies of (b) Model-(DA)-T1', and (c) Model-(Fixmatch)-T1' on Dataset-S and Unlabeled dataset-T1' at the 1~10 training epochs.

validation set for model selecting. Noted that the real labels are assigned to Unlabeled dataset-T1', to evaluate the recognition performance of historical models. As shown in Fig. 7(a), the accuracies of pseudo labels created by EPL method are all above 97% in three training times, which proves that EPL method can create a high-quality pseudo-label dataset. Then, the accuracies of Model-(DA)-T1' in three training times are sorted in Fig. 7(b), where each training uniformly achieves the models of 100 epochs. The accuracy positions of three selected models are marked in red boxes, whose sites are all above 95%, and the accuracies of three selected models are all above 98%. It indicates the EPL method can stably select an adaptive model, which is crucial for practical applications when labeled data is not available in target domain.

Model transferring from Domain-S to other domains

Performance evaluation on domain differences

As shown in Fig. 8(a), based on Model-(Baseline) and two unlabeled datasets, Model-(ADAI)-T1' and Model-(ADAI)-T2' are achieved by ADAI scheme. Compared with the accuracies of Model-(Baseline) on Dataset-T1 and Dataset-T2, the accuracies of Model-(ADAI)-T1' and Model-(ADAI)-T2' are improved by 33.2% and 73%, respectively. It proves that ADAI scheme can improve the overall accuracy of recognition model on each target domain. Then, the reduction of MAR and FAR by ADAI scheme on Domain-T1 and Domain-T2 are respectively shown in Fig. 8(b, c). The Model-(ADAI)-T1' achieves the MAR of 1.4% and FAR of 4.3% on Dataset-T1, respectively, which are both smaller than that of Model-(Baseline). Similarly, the MAR and FAR of Model-(ADAI)-T2' on Dataset-T2 are 2.7% and 0%, respectively, which are reduced by 60.8% and 9.8% when compared with that of Model-(Baseline). Overall, ADAI scheme can improve model adaptability for the corresponding domain by utilizing information contained in unlabeled dataset.

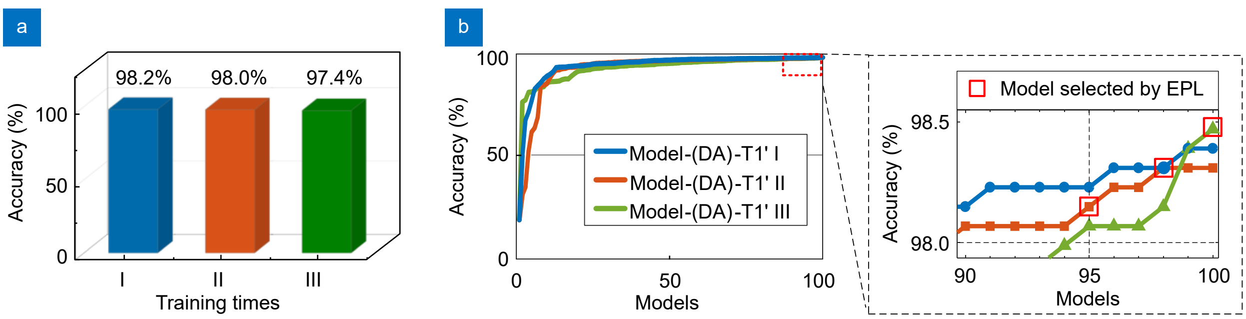

Fig. 7 | (**a**) Accuracies of pseudo labels created by EPL method in three training times. (**b**) Performance of EPL method for model selecting.

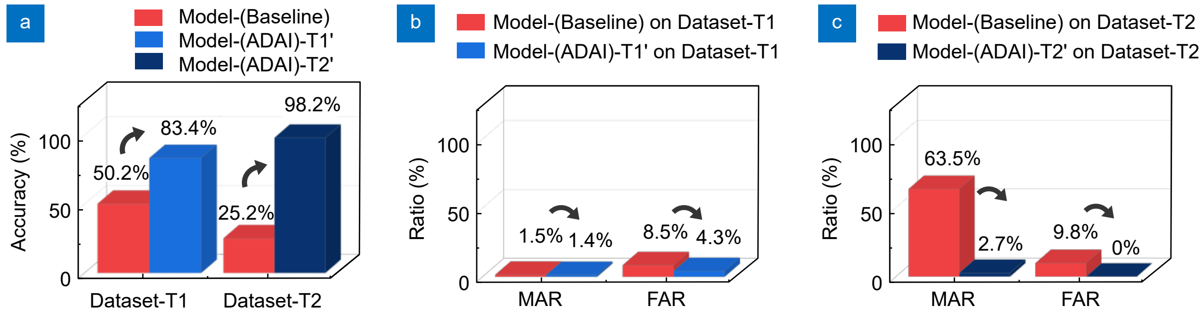

Fig. 8 | (**a**) The accuracies of Model-(Baseline), Model-(ADAI)-T1', and Model-(ADAI)-T2' on Dataset- T1 and Dataset-T2. The MAR and FAR of (**b**) Model-(Baseline) and Model-(ADAI)-T1' on Dataset-T1, and (**c**) Model-(Baseline) and Model-(ADAI)-T2' on Dataset-T2, respectively.

Additionally, the confusion matrices of Model-(Baseline), Model-(ADAI)-T1' and Model-(ADAI)-T2' on two datasets are compared. As shown in Fig. 9(a, b), Model-(Baseline) performs poorly on Dataset-T1 and Dataset-T2, especially the performance on samples of background noise. It reveals the significant deviations in data distribution between Domain-S and other target domains. To narrow this deviation, ADAI scheme is used to mine more information from two unlabeled datasets. As shown in Fig. 9(c, d), Model-(ADAI)-T1' and Model-(ADAI)-T2' significantly improve overall recognition performance of four events on corresponding domains when compared with Model-(Baseline). These improvements are attributed to the additional information contained in non-intrusive samples from two unlabeled datasets. Since there are no unlabeled samples corresponding to intrusion events in target domain, ADAI may not learn the effective information about intrusion events, which may perform poorly in some types of events, such as the event-3 on Dataset-T1. To improve the accuracy of these intrusion events, expanding unlabeled datasets and improving their quality is considered in future work. Furthermore, a simulated experimental field and corresponding mathematical model will be explored to collect data, which can simulate sensing processes, such as sound excitation, sound propagation, and fiber sensing. To tackle the new types of events in target domain, incremental learning and GMM will be applied as the supplement to ADAI scheme, which can retain knowledge of events type in Domain-S and Domain-T.

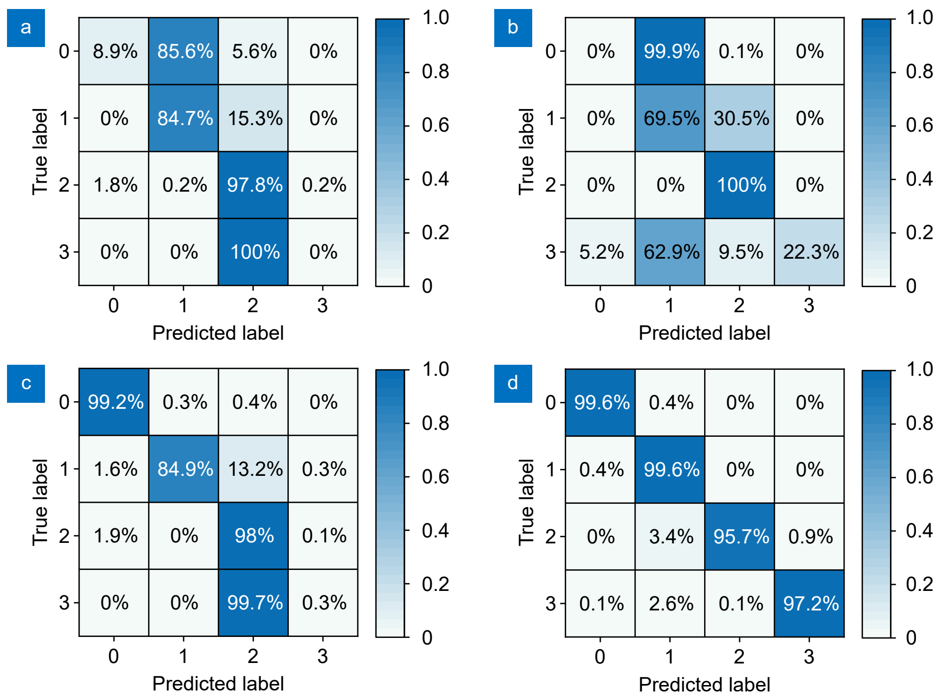

Fig. 9 | The confusion matrices of (**a**) the Model-(Baseline) on Dataset-T1, (**b**) the Model-(Baseline) on Dataset-T2, (**c**) the Model-(ADAI)-T1' on Dataset-T1, and (**d**) the Model-(ADAI)-T2' on Dataset-T2.

Robustness evaluation

Based on the statistical amplitude of 0.02 for background noise, Gaussian noise of the amplitude 0.02 is added to each sample with the ratios from 0% to 100%. To simulate condition of information loss, each sample is shifted with the points of [−250, −125, 0, 125, 250] on the time axis, where −250 means that the sample of length 1000 is shifted left by 250 points. The accuracies of Model-(ADAI)-T1' and Model-(ADAI)-T2' on two datasets under the conditions of different time-shift points and noise of different ratios are shown in Fig. 10(a) and (b), respectively. The accuracies of two models decrease by up to 3% and 7%, respectively, which are within the acceptable range for robustness. As the noise ratio increases, the overall accuracies of both models decrease. While the accuracy trends of these two models are different when facing time-shift, which is due to the differences in time-shift characteristics between two datasets.

The ROC curves of Model-(ADAI)-T1' and Model-(Baseline) on Dataset-T1 are shown in Fig. 11(a), where two models both perform well on Dataset-T1 with the AUC value of 0.996 and 0.995, respectively. However, as demonstrated in Fig. 11(b), the AUC value of Model-(Baseline) on Dataset-T2 drops to 0.812 and the AUC of Model-(ADAI)-T1' rises to 1, which further proves the robustness of ADAI scheme.

Ablation study about model transferring with labeled Dataset-T1

To improve the recognition performance of model on intrusion events, labeled samples are needed. In some cases, the number of acquired labeled samples in target domain is unpredictable. Thus, the recognition performance of Model-(ADAI)-T1'-T1, Model-(Baseline)-T1, and Model-(AE)-T1'-T1 are compared when providing different numbers of labeled samples from Domain-T1. As depicted in Fig. 12(a), the Model-(ADAI)-T1'-T1 consistently achieves the highest

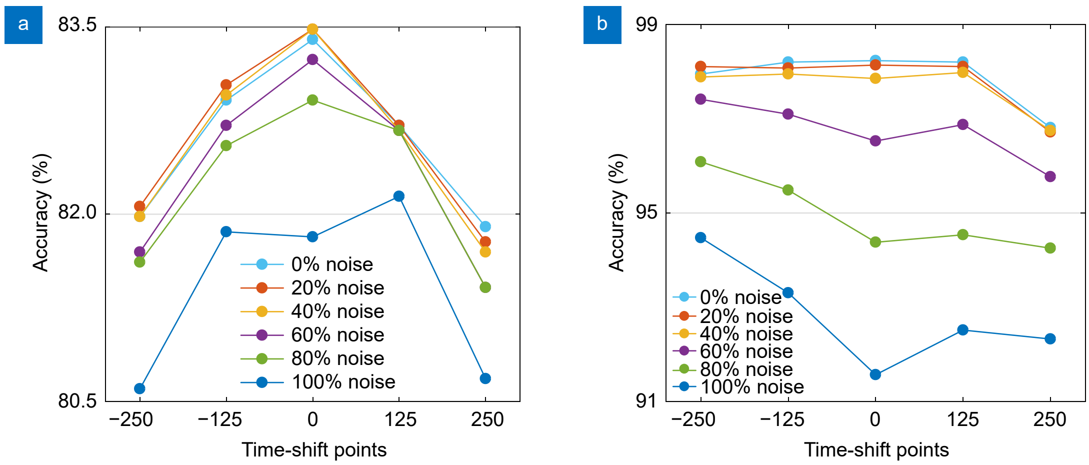

Fig. 10 | The accuracies of (a) Model-(ADAI)-T1' on Dataset-T1, and (b) Model-(ADAI)-T2' on Dataset-T2 under the conditions of different time-shift points and different ratio noise.

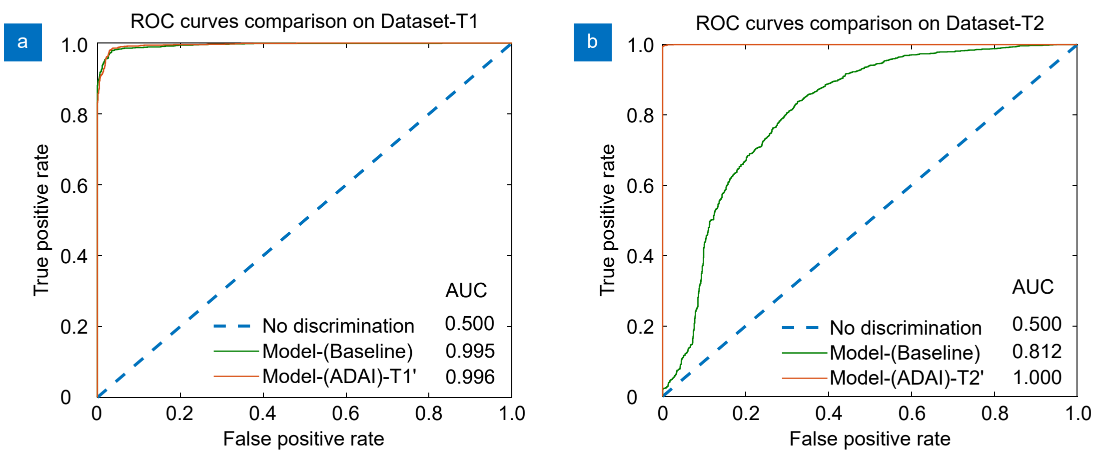

Fig. 11 | The comparison of ROC curves between ADAI scheme and Baseline on (a) Dataset-T1, and (b) Dataset-T2.

accuracy. Its accuracy reaches 93.7% when provided with only three samples for each class, proving the robustness of ADAI scheme. Compared with the Model-(ADAI)-T1'-T1, the Model-(Baseline)-T1 achieves significantly lower accuracy when the number of labeled samples is limited to 1 to 8. As for the Model-(AE)-T1'-T1, its recognition accuracy is lower than that of other models, especially when the number of labeled samples is 32 or fewer. Overall, the ADAI scheme not only incorporates model knowledge from Domain-S but also leverages data information from two domains. Consequently, Model-(ADAI)-T1'-T1 learns more information than Model-(Baseline)-T1 and Model-(AE)-T1'-T1, enabling its significant advantage when trained with labeled samples. Furthermore, the t-distributed stochastic neighbor embedding (T-SNE) visualizations of above three models are compared when four labeled samples for each class are provided. As depicted in Fig. 12(b–d), the Model-(ADAI)-T1'-T1 exhibits good intra-class compactness and inter-class separability. While the Model-(Baseline)-T1 shows poor intra-class compactness, in which the samples of same class are distributed across different regions in T-SNE figure. And its inter-class separability is also inferior to the Model-(ADAI)-T1'-T1. The visualization result of Model-(AE)-T1'-T1 indicates that it lacks recognition capability.

The number of samples required for a satisfied accuracy is crucial in practical applications. As shown in Table 2, to reach the accuracy levels of 85%, 90%, and 95%, the Model-(ADAI)-T1'-T1 requires at least 2, 3, and 4 samples for each class, respectively. While, the Model-(Baseline)-T1 necessitates four times more samples than the Model-(DA)-T1'-T1 when achieving the equivalent recognition accuracy. Additionally, the Model-(AE)-T1'-T1 needs a minimum of 64 samples for each class to achieve the recognition accuracy of 85%. These results further demonstrate that ADAI scheme can effectively incorporate knowledge from two domains, thereby reducing dependence of model training on the number of labeled samples.

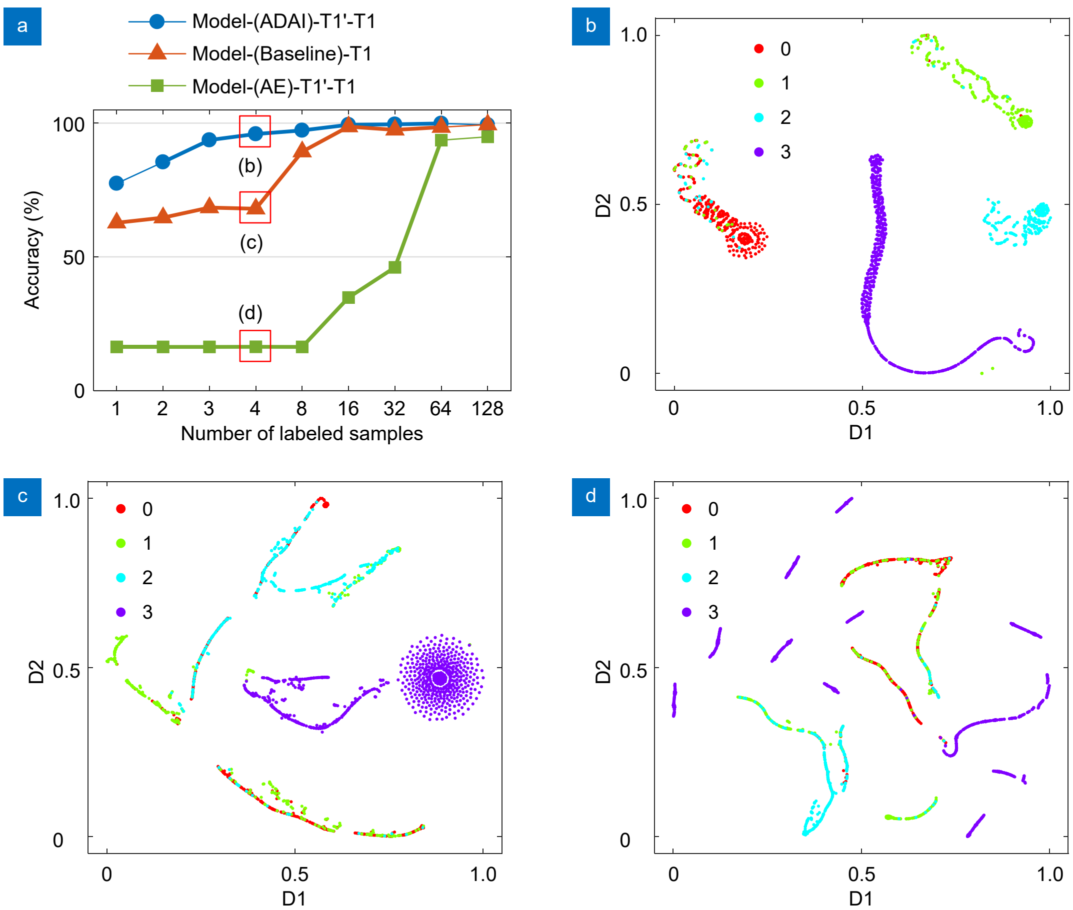

Fig. 12 | (a) The performance comparison of Model-(ADAI)-T1'-T1, Model-(Baseline)-T1, and Model-(AE)-T1'-T1 when providing different number of labeled samples from Domain-T1. The T-SNE visualizations of the (b) Model-(ADAI)-T1'-T1, (c) Model-(Baseline)-T1, and (d) Model-(AE)-T1'-T1 when providing four labeled samples for each class.

Table 2 | Number of required samples for each class of Model-(AE)-T1'-T1, Model-(Baseline)-T1, and Model-(ADAI)-T1'-T1 at different accuracy levels.

Accuracy to be achieved	Model-(AE)-T1'-T1	Model-(Baseline)-T1	Model-(ADAI)-T1'-T1
85%	64	8	2
90%	64	16	3
95%	128	16	4

Conclusions

In this paper, an ADAI scheme for signal recognition of DSS is proposed. By fine-tuning pre-trained model with the existing labeled and unlabeled data in each domain, ADAI scheme can train a series of adaptive AI models for all target domains, significantly reducing the FAR and MAR of DSS. The experiment of intrusion signal recognition with DOFS system is conducted to demonstrate the efficacy of ADAI scheme, showcasing a FAR of merely 4.3% and 0%, along with a MAR of only 1.4% and 2.7% within two specific target domains. An ablation study about model transferring with labeled dataset is further employed to prove the robustness of ADAI scheme. The ADAI scheme is expected to offer a practical paradigm for signal recognition of DSS in multiple application fields.

References

1. Abdollahzadeh S, Navimipour NJ. Deployment strategies in the wireless sensor network: a comprehensive review. *Comput Commun* **91**–**92**, 1–16 (2016).
2. Johnson KJ, Rose-Pehrsson SL. Sensor array design for complex sensing tasks. *Annu Rev Anal Chem* **8**, 287–310 (2015).
3. Li J, Bao RR, Tao J et al. Recent progress in flexible pressure sensor arrays: from design to applications. *J Mater Chem C* **6**, 11878–11892 (2018).
4. Wang HT, Hao CL, Lin H et al. Generation of super-resolved optical needle and multifocal array using graphene oxide metalenses. *Opto-Electron Adv* **4**, 200031 (2021).
5. Hürlimann M, Coviello V, Bel C et al. Debris-flow monitoring and warning: review and examples. *Earth-Sci Rev* **199**, 102981 (2019).
6. Kandris D, Nakas C, Vomvas D et al. Applications of wireless sensor networks: an up-to-date survey. *Appl Syst Innov* **3**, 14 (2020).
7. Zhu WQ, Biondi E, Li JX et al. Seismic arrival-time picking on distributed acoustic sensing data using semi-supervised learning. *Nat Commun* **14**, 8192 (2023).
8. Yang HY, Wang YC, Peng HY et al. Breath biopsy of breast cancer using sensor array signals and machine learning analysis. *Sci Rep* **11**, 103 (2021).
9. Leal-Junior A, Avellar L, Biazi V et al. Multifunctional flexible optical waveguide sensor: on the bioinspiration for ultrasensitive sensors development. *Opto-Electron Adv* **5**, 210098 (2022).
10. Hou LQ, Bergmann NW. Novel industrial wireless sensor networks for machine condition monitoring and fault diagnosis. *IEEE Trans Instrum Meas* **61**, 2787–2798 (2012).
11. Krantz-Rülcker C, Stenberg M, Winquist F et al. Electronic tongues for environmental monitoring based on sensor arrays and pattern recognition: a review. *Anal Chim Acta* **426**, 217–226 (2001).
12. Zheng XT, Yang ZJ, Sutarlie L et al. Battery-free and AI-enabled multiplexed sensor patches for wound monitoring. *Sci Adv* **9**, eadg6670 (2023).
13. Alsheikh MA, Lin SW, Niyato D et al. Machine learning in wireless sensor networks: algorithms, strategies, and applications. *IEEE Commun Surv Tut* **16**, 1996–2018 (2014).
14. Lee H, Lee S, Kim J et al. Stretchable array electromyography sensor with graph neural network for static and dynamic gestures recognition system. *npj Flex Electron* **7**, 20 (2023).
15. Ding Y, Elsayed EA, Kumara S et al. Distributed sensing for quality and productivity improvements. *IEEE Trans Autom Sci Eng* **3**, 344–359 (2006).
16. Duan LX, Xu D, Tsang IWH. Domain adaptation from multiple sources: a domain-dependent regularization approach. *IEEE Trans Neural Netw Learn Syst* **23**, 504–518 (2012).
17. Quqa S, Li SJ, Shu YN et al. Crack identification using smart paint and machine learning. *Struct Health Monit* **23**, 248–264 (2024).
18. Kim KK, Kim M, Pyun K et al. A substrate-less nanomesh receptor with meta-learning for rapid hand task recognition. *Nat Electron* **6**, 64–75 (2023).
19. Liu SQ, Yu FH, Hong R et al. Advances in phase-sensitive optical time-domain reflectometry. *Opto-Electron Adv* **5**, 200078 (2022).
20. Lyu CG, Hu XY, Niu ZH et al. A light-weight neural network for marine acoustic signal recognition suitable for fiber-optic hydrophones. *Exp Syst Appl* **235**, 121235 (2024).
21. Xin LP, Li ZY, Gui X et al. Surface intrusion event identification for subway tunnels using ultra-weak FBG array based fiber sensing. *Opt Express* **28**, 6794–6805 (2020).
22. Tejedor J, Macias-Guarasa J, Martins HF et al. A contextual GMM-HMM smart fiber optic surveillance system for pipeline integrity threat detection. *J Lightw Technol* **37**, 4514–4522 (2019).
23. Wu HJ, Liu XR, Xiao Y et al. A dynamic time sequence recognition and knowledge mining method based on the hidden markov models (HMMs) for pipeline safety monitoring with Φ-OTDR. *J Lightw Technol* **37**, 4991–5000 (2019).
24. Zhang SX, He T, Li H et al. Modified data augmentation integration method for robust intrusion events recognition with fiber optic DAS system. *J Lightw Technol* **42**, 453–462 (2024).
25. Shiloh L, Eyal A, Giryes R. Efficient processing of distributed acoustic sensing data using a deep learning approach. *J Lightw Technol* **37**, 4755–4762 (2019).
26. Shi Y, Dai SW, Liu XY et al. Event recognition method based on dual-augmentation for a Φ-OTDR system with a few training samples. *Opt Express* **30**, 31232–31243 (2022).

27. Huang XD, Wang BY, Liu K et al. An event recognition scheme aiming to improve both accuracy and efficiency in optical fiber perimeter security system. *J Lightw Technol* **38**, 5783–5790 (2020).
28. Lyu CG, Huo ZQ, Liu YG et al. Robust intrusion events recognition methodology for distributed optical fiber sensing perimeter security system. *IEEE Trans Instrum Meas* **70**, 9505109 (2021).
29. Yang F, Ling ZN, Zhang YH et al. Event detection, localization, and classification based on semi-supervised learning in power grids. *IEEE Trans Power Syst* **38**, 4080–4094 (2023).
30. Li YJ, Cao XM, Ni WH et al. A deep learning model enabled multi-event recognition for distributed optical fiber sensing. *Sci China Inf Sci* **67**, 132404 (2024).
31. Wu HJ, Gan DK, Xu CR et al. Improved generalization in signal identification with unsupervised spiking neuron networks for fiber-optic distributed acoustic sensor. *J Lightw Technol* **40**, 3072–3083 (2022).
32. Wang SL, Liu F, Liu B. Semi-supervised deep learning in high-speed railway track detection based on distributed fiber acoustic sensing. *Sensors* **22**, 413 (2022).
33. Yang YY, Zhang HF, Li Y. Long-distance pipeline safety early warning: a distributed optical fiber sensing semi-supervised learning method. *IEEE Sens J* **21**, 19453–19461 (2021).
34. Shi Y, Li YH, Zhang YC et al. An easy access method for event recognition of Φ-OTDR sensing system based on transfer learning. *J Lightw Technol* **39**, 4548–4555 (2021).
35. Lyu CG, Huo ZQ, Cheng X et al. Distributed optical fiber sensing intrusion pattern recognition based on GAF and CNN. *J Lightw Technol* **38**, 4174–4182 (2020).
36. Ben-David S, Blitzer J, Crammer K et al. A theory of learning from different domains. *Mach Learn* **79**, 151–175 (2010).
37. Borgwardt KM, Gretton A, Rasch MJ et al. Integrating structured biological data by kernel maximum mean discrepancy. *Bioinformatics* **22**, e49–e57 (2006).
38. Tzeng E, Hoffman J, Zhang N et al. Deep domain confusion: maximizing for domain invariance. arXiv: 1412.3474, 2014. https://arxiv.org/abs/1412.3474
39. Scudder H. Probability of error of some adaptive pattern-recognition machines. *IEEE Trans Inf Theory* **11**, 363–371 (1965).
40. McLachlan GJ. Iterative reclassification procedure for constructing an asymptotically optimal rule of allocation in discriminant analysis. *J Am Stat Assoc* **70**, 365–369 (1975).
41. Tarvainen A, Valpola H. Mean teachers are better role models: weight-averaged consistency targets improve semi-supervised deep learning results. In *Proceedings of the 31st International Conference on Neural Information Processing Systems* 1195–1204 (Curran Associates Inc. , 2017). https://dl.acm.org/doi/10.5555/3294771.3294885
42. Lu YL, Zhu T, Chen L et al. Distributed vibration sensor based on coherent detection of phase-OTDR. *J Lightw Technol* **28**, 3243–3249 (2010).
43. Sohn K, Berthelot D, Li CL et al. FixMatch: simplifying semi-supervised learning with consistency and confidence. In *Proceedings of the 34th International Conference on Neural Information Processing Systems* 51 (Curran Associates Inc. , 2020). https://dl.acm.org/doi/10.5555/3495724.3495775
44. Masci J, Meier U, Cireşan D et al. Stacked convolutional auto-encoders for hierarchical feature extraction. In *Proceedings of the 21st International Conference on Artificial Neural Networks and Machine Learning–ICANN 2011* 52–59 (Springer, 2011); https://doi.org/10.1007/978-3-642-21735-7_7.

Acknowledgements

We are grateful for financial supports from the National Natural Science Foundation of China (NSFC) (No. 61922033 & U22A20206); and Zhejiang Provincial Market Supervision Bureau Young Eagle Plan project under Grant CY2022228.

Author contributions

S. X. Zhang, H. Li and Q. Z. Sun proposed the original idea of the project. Q. Z. Sun supervised the project. C. Z. Fan, Z. J. Yan and D. M. Liu participated the discussion of the research. S. X. Zhang, Z. C. Zeng, J. Wu, and C. Xiong carried out the experiments and collected the data. S. X. Zhang and H. Li analyzed all the data. S. X. Zhang and Q. Z. Sun wrote the paper. All authors discussed the results and commented on the manuscript.

Competing interests

The authors declare no competing financial interests.

Supplementary information

Supplementary information for this paper is available at https://doi.org/10.29026/oea.2024.240119

Scan for Article PDF